

# Molecular simulation and experimental studies of the miscibility of polylactic acid/polyethylene glycol blends

Adisak Takhulee<sup>1</sup> · Yoshiaki Takahashi<sup>2</sup> · Visit Vao-soongnern<sup>1</sup>

Received: 7 June 2016 / Accepted: 19 December 2016 / Published online: 27 December 2016  
© Springer Science+Business Media Dordrecht 2016

**Abstract** Computer simulation and experiments were performed to investigate the miscibility of PLA/PEG blends with different PEG concentrations. Flory-Huggins interaction ( $\chi$ ) parameter used to predict the miscibility for the blends was estimated by molecular dynamic simulation of fully atomistic model. The calculated  $\chi$  parameter and radial distribution function suggest that the PLA and PEG blends are likely miscible at low PEG concentrations (10–30 wt%), but they become apparently immiscible at higher PEG content (>50 wt%). This result is consistent with density distribution of PLA and PEG beads calculated from dissipative particle dynamics simulation of coarse-grained model. To support the computational results, experiments based on differential scanning calorimetry (DSC) and rheometry were also performed. The DSC thermograms of 90:10, 80:20, and 70:30 (wt/wt) of PLA/PEG blends showed a single glass transition and PLA melting peak, indicating PLA/PEG is miscible over this composition. In rheometry, frequency ( $\omega$ ) dependence of storage moduli ( $G'$ ) at low frequencies for 75:25 and 70:30 blends indicate that these samples are near the phase separation point.

**Keywords** Molecular dynamic simulation · Dissipative particle dynamics simulation · Polymer blends · Poly(lactic acid) · Poly(ethylene glycol)

✉ Visit Vao-soongnern  
visit@sut.ac.th

<sup>1</sup> Laboratory of Computational and Applied Polymer Science, School of Chemistry, Institute of Science, Suranaree University of Technology, Nakhon Ratchasima 30000, Thailand

<sup>2</sup> Evaluation Office of Materials Properties, Institute for Materials Chemistry and Engineering, Kyushu University, Kasuga, Fukuoka 816-8580, Japan

## Introduction

Poly(lactic acid) (PLA) is a biodegradable polymer which can be produced from renewable resources. It has been expected to replace the petroleum base polymers because of its excellent properties, such as nontoxic good mechanical properties and biodegradability. PLA has potential use in a wide array of applications, such as biomedical and pharmaceutical fields and food packaging [1, 2]. However, PLA has not been extensively used, especially in the application to flexible materials because of its brittleness, low crystallization rate, and lower impact resistance at room temperature. To address these major disadvantages, various strategies including addition of low molecular weight plasticizers, copolymerization, and melt blending with flexible polymers or rubbers have been extensively studied by various experimental techniques [3–6]. Compared with other methods to increase material flexibility, plasticization appears more industrially practical due to its cost-effectiveness and high efficiency. Various low molecular weight compounds have been investigated as the potential plasticizers for PLA [7–10].

PEG is a promising plasticizer for PLA because of its biocompatibility, low cost, and efficiency to improve the ductility and flexibility of PLA [9, 11]. A number of experiments were conducted to investigate the compatibility of the PLA/PEG blends. Although PEG appeared to be an effective plasticizer for PLA, it was reported that the blends become unstable with time because of the slow phase separation caused by crystallization of PEG from homogeneous blends even at room temperature [7, 8, 12, 13]. To study the effect of PEG composition and molecular weight on PLA/PEG miscibility, Sheth et al. [14] concluded from differential scanning calorimetry (DSC), polarized optical microscopy, and dynamic mechanical analysis that PLA ( $140,000 \text{ g mol}^{-1}$ )/PEG

(2000 g mol<sup>-1</sup>) blends are miscible in compositions less than 50:50 (wt/wt). Younes and Cohn [15] studied the phase separation of the PLA/PEG blends with different PEG molecular weights (1500, 3400, 6000 and 35,000 g mol<sup>-1</sup>) by DSC and infrared spectroscopy. They reported that whenever one of the components is more than 20% by weight, it is able to crystallize; such blends consist of two semi-miscible crystalline phases dispersed in an amorphous matrix due to the enhanced crystallizability of the longer PEG chains. It was suggested that crystallization phenomena are a driving force for this microphase segregation.

Despite the above-mentioned experimental studies, the miscibility of PLA/PEG blends remains elusive at the molecular level. The crystallization kinetics seems to strongly affect the experimental studies. With the ever-growing computational power and resources, molecular simulations have played increasingly important role in material modeling and subsequent technology development, as they can reveal the microscopic pictures of underlying mechanisms that are otherwise experimentally inaccessible or difficult to obtain. Molecular dynamic (MD) simulation has been applied to study multiphase polymer systems providing a bridge between models and experiments. However, the broad range of time scales and underlying structure prohibits the fully atomistic simulation method that captures all of these processes. Some alternative methods have been developed to overcome these problems. The coarse-graining model or mesoscale method has been successful in extending this scope. In this model, about four to five carbon atoms in a polymer chain are grouped into a single bead, and thus, many states can be easily generated and equilibrated. One example is the dissipative particle dynamics (DPD), a mesoscale simulation technique developed to model Newtonian and non-Newtonian fluids [16]. It is capable to investigate the phase morphology and interface properties of multiphase systems. During the past decade, both atomistic MD and mesoscale DPD simulation were applied to calculate the polymer–polymer interaction and to predict the miscibility of polymer blends [17–28].

In this work, computer simulation based on a combination of atomistic and mesoscale simulation was employed to investigate the miscibility and phase separation characteristics of PLA/PEG blends. First, MD simulation of the fully atomistic model was performed to study the miscibility of the PLA/PEG blends by determining Flory-Huggins ( $\chi$ ) interaction parameter and the radial distribution function. Then, DPD simulation of the mesoscale model was employed to investigate the phase separation. The results are partly confirmed by experiments based on rheometry and differential scanning calorimetry (DSC).

## Computer simulation

### MD simulation

The miscibility state at the molecular level of PLA/PEG blends was investigated by MD simulation of fully atomistic model. The Condensed Phase Optimized Molecular Potentials for Atomistic Simulation Studies (COMPASS) force field was used for computing all intra- and inter-molecular interactions. The total potential energy ( $E_{\text{pot}}$ ) was expressed as:

$$E_{\text{pot}} = E_{\text{valence}} + E_{\text{cross}} + E_{\text{nonbond}} \quad (1)$$

The energy of valence or bonded interaction ( $E_{\text{valence}}$ ) comprises the bond stretching energy ( $E_{\text{bond}}$ ), valence angle bending energy ( $E_{\text{angle}}$ ), dihedral angle torsion energy ( $E_{\text{torsion}}$ ), and inversion energy (also called out of plane interaction denoted as  $E_{\text{inversion}}$  or  $E_{\text{oop}}$ ) terms. The energy of cross-term ( $E_{\text{cross}}$ ) was used to account for bond or angle distortions caused by nearby atoms. These terms are required to accurately reproduce vibrational frequencies and the dynamic properties of molecules. Finally, the nonbond interaction term ( $E_{\text{nonbond}}$ ) accounts for the interaction between non-bonded atoms and includes the van der Waals energy ( $E_{\text{vdw}}$ ), the Coulomb electrostatic energy ( $E_{\text{coulomb}}$ ), and the hydrogen bond energy ( $E_{\text{H-bond}}$ ).

PLA and PEG chains were first generated from LA and EG repeating units, respectively, using the rotational isomeric state (RIS) model [29] which describes the conformational characteristics of the unperturbed molecules. The cubic simulation boxes were then constructed with the Amorphous Cell module based on the packing technique of Theodorou and Suter [30] and Meirovitch scanning method [31]. The polymer density in a simulation box corresponds to the bulk density of each polymer, i.e., PLA = 1.206 g cm<sup>-3</sup> and PEG = 1.127 g cm<sup>-3</sup>. To avoid the long simulation time, the optimized chain lengths of 30 and 50 repeating units for PLA and PEG, respectively, were set based on constant solubility parameters ( $\delta$ ) for each polymer with varying the number of repeating units [19, 20].

After the amorphous polymer structure was constructed in the simulation box, energy minimization was subsequently carried out to eliminate the local non-equilibrium structures with the convergence threshold of 0.001 kcal mol<sup>-1</sup> Å<sup>-1</sup>. The MD simulation was then performed at 500 K and 1 bar for 2 ns in the NPT ensemble. Here, the temperature was chosen with 500 K to ensure that polymers are in the molten (amorphous) state (melting temperature ( $T_m$ ) of PLA : 433–453 K,  $T_m$  of PEG : about 333 K. In order to further relax local hot spots and to allow the system to achieve equilibrium, the polymer structures were subjected to a 10-circle thermal annealing from 300 to 1000 K and then back to 300 K with 50 K intervals. At each

temperature, 100 ps of NPT MD simulation was performed at the constant pressure (1 bar) with a time step of 1 fs. After the 10-circle annealing, the 2 ns for NVT MD simulation was carried out at constant volume. At the last stage, 1 ns of NVT MD simulation was performed to collect the data for analysis. The parameters of MD simulations for PLA/PEG blends are displayed in Table 1.

MD simulation of this fully atomistic model was then employed to predict the miscibility of PLA/PEG with different PEG concentration. The miscibility of polymer blends was calculated by examining the Flory-Huggins parameter ( $\chi_{ij}$ ) calculated according to:

$$\chi_{ij} = \left( \frac{\Delta E_{\text{mix}}}{RT} \right) V_m \tag{2}$$

where  $V_m$  is the molar volume of the repeating unit chosen as a reference.  $V_m$  of PLA was selected to be used as a reference in this study ( $57.7 \text{ cm}^3 \text{ mol}^{-1}$ ),  $R$  is the molar gas constant, and  $T$  is the temperature of the simulation in Kelvin. The energy of mixing,  $\Delta E_{\text{mix}}$ , can be calculated according to:

$$\Delta E_{\text{mix}} = \varphi_A \left( \frac{E_{\text{coh}}}{V} \right)_A + \varphi_B \left( \frac{E_{\text{coh}}}{V} \right)_B - \varphi_{\text{mix}} \left( \frac{E_{\text{coh}}}{V} \right)_{\text{mix}} \tag{3}$$

where the terms in the parentheses represent the cohesive energies ( $E_{\text{coh}}/V$ ) of the pure polymers (A and B) and the blend (mix) and  $\phi_A$  and  $\phi_B$  represent volume fractions of PLA and PEG, respectively, in the blend.

### DPD simulation

DPD simulation, introduced by Hoogerbrugge and Koelman [32], is a mesoscale method for simulating coarse-grained systems over a longer length and time scales. In DPD simulation, several atoms or repeating units are grouped together into a single bead. The polymer chains in DPD simulation can be

considered to consist of number of beads ( $N_{\text{DPD}}$ ) which is calculated from:

$$N_{\text{DPD}} = \frac{M_p}{M_m C_n} = \frac{N}{C_n} \tag{4}$$

where  $M_p$  is molar mass of polymers,  $M_m$  is molar mass of repeating units,  $C_n$  is characteristic ratio, and  $N$  is number of repeating units. The characteristic ratio ( $C_n$ ) of the polymer can be estimated using the Synthia module in Materials Studios software. The  $C_n$  values for PLA and PEG are 3.40 and 4.98, respectively.

The force acting on a bead is a sum of three pairwise contributions, that is, a conservative force ( $f^C$ ), a dissipative force ( $f^D$ ), and a random force ( $f^R$ ) as:

$$f_i = \sum_{j \neq i} (f_{ij}^C + f_{ij}^D + f_{ij}^R) \tag{5}$$

where the sum runs over all other particles within a certain cutoff radius ( $r_c$ ). As this is the only length scale in the system, we use the cutoff radius as our unit of length,  $r_c = 1$ . The bead interactions ( $a_{ij}$ ) of DPD can be mapped onto Flory-Huggins theory through the  $\chi$  parameter [33] as:

$$a_{ij} = a_{ii} + 3.27\chi_{ij} \tag{6}$$

$$\chi_{ij} = \frac{V_{ij}(\delta_i - \delta_j)^2}{RT} \tag{7}$$

where  $V_{ij}$  is the arithmetic average of molar volumes of beads  $i$  and  $j$ .  $\delta_i$  and  $\delta_j$  are the solubility parameters of beads  $i$  and  $j$ , respectively, which depend on the chemical nature of each species. The interaction parameter between the same type beads  $a_{ii}$  equals 25. The values of  $\chi_{ij}$  parameter at 300 K for DPD simulation were obtained from MD simulation. The procedure for calculating the  $\chi_{ij}$  parameter was described in MD simulation section. The  $\chi_{ij}$  parameter is put into Eq. (6), and the interaction in the DPD simulation is obtained.

**Table 1** The parameters of MD simulations for PLA/PEG blends at 300 K

System	LA units	EG units	Number of chains	Composition (wt% PLA)	Density ( $\text{g cm}^{-3}$ )
PLA	30	–	1 PLA	100	1.206
PEG	–	50	1 PEG	–	1.127
PLA/PEG 90:10	30	50	9PLA/1PEG	90	1.198
PLA/PEG 80:20	30	50	4PLA/1PEG	80	1.190
PLA/PEG 70:30	30	50	7PLA/3PEG	70	1.180
PLA/PEG 75:25	30	50	3PLA/1PEG	75	1.186
PLA/PEG 50:50	30	50	1PLA/1PEG	50	1.167
PLA/PEG 30:70	30	50	3PLA/7PEG	30	1.151
PLA/PEG 20:80	30	50	1PLA/4PEG	20	1.143
PLA/PEG 10:90	30	50	1PLA/9PEG	10	1.135

DPD simulation of PLA/PEG was performed in a simulation cell with the bead density ( $\rho$ ) of 3. The simulation box size is  $30 \times 30 \times 30$  with periodic boundary conditions in three directions. The simulations were performed at reduced temperature ( $k_B T = 1$ ); this allows a reasonable and efficient relaxation for each binary blend. A total of  $10^5$  time steps with step size  $\Delta t = 0.05$  in DPD reduced units are performed for equilibration. The molecular weight of 100,000 and 8000  $\text{g mol}^{-1}$  for PLA and PEG homopolymers, respectively, were employed for DPD simulation to compare with experimental study. The number of beads per chain of PLA and PEG, blend composition, and bead–bead pair interaction parameter for DPD simulation are shown in Table 2.

## Experimental

### Materials

The commercial grade PLA (PLA 2002D, Nature Work) and PEG (PEG8k, Aldrich) are used without further purification in this study. Molecular weights ( $M_w$ ) and molecular weight distribution (MWD) of PLA and PEG were determined by gel permeation chromatography using Shimadzu LC 20A equipped with the reflective index detector, RID-10A. A PLgel 5 mm diameter MIXED-D column with a guard column was used. The measurement was operated at 40 °C using tetrahydrofuran (THF) as a mobile phase with flow rate of 0.5 ml/min. In 15 mg/ml of polymer in THF, 40  $\mu\text{l}$  was injected for each analysis. Molecular weights of the polymers were obtained relative to polystyrene (PS) standards (PLA:  $M_w = 8.2 \text{ kg mol}^{-1}$  and MWD = 1.24, PEG:  $M_w = 118 \text{ kg mol}^{-1}$  and MWD = 1.27).

Prior to blending, PLA and PEG were dried at 50 °C in vacuum oven for 24 h. The mixture compositions of PLA/PEG with 90:10, 80:20, 70:30, 75:25, and 50:50 were prepared by solution casting. The solutions of PLA and PEG (5% w/v) were prepared by dissolving each polymer

into dichloromethane. Each solution was then mixed together. The solutions were cast on glass Petri dishes, and the solvent was allowed to evaporate at room temperature. All obtained films were further dried overnight under vacuum at room temperature to eliminate residual solvent.

### Measurements

DSC thermograms of polymers were recorded on Pyris Diamond (Perkin-Elmer) with nitrogen as the purge gas. An indium standard was used for the calibration. Samples of 5.0–8.0 mg were loaded into aluminum pans, and the pans were sealed prior to measurement. The sample was first heated from 0 to 180 °C with a heating rate of 10 °C  $\text{min}^{-1}$  and held at 180 °C for 5 min to delete thermal history. After that, the sample was cooled down to 0 °C with a cooling rate of 100 °C/min (referred as quenched sample) and held at 0 °C for 1 min. The second run was performed by heating the sample to 180 °C with a heating rate of 10 °C  $\text{min}^{-1}$ . To examine the effect of cooling rate, slowly cooled sample, from 180 to 0 °C with a cooling rate of 10 °C/min, was also measured by the second run. Glass transition temperature ( $T_g$ ), the crystallization temperature ( $T_c$ ), the degree of crystallinity ( $X_c$ ), and the melting temperature ( $T_m$ ) were determined in the second heating scan.

Rheological measurements were carried out in a rheometer (Anton Parr MCR300) equipped with a parallel plate geometry with a diameter of 8 mm. All measurements were performed under nitrogen atmosphere. PLA and PEG with different compositions, 90:10, 85:15, 80:20, 75:25, and 70:30 (wt/wt) were investigated. The samples were dried in a vacuum oven for 24 h before the measurement. The sample disks were melted at predetermined temperature for 5 min in parallel plates to eliminate the residual thermal history before the measurements. Dynamic strain sweep tests were carried out to obtain the linear region of response. Frequency sweep tests were carried out in the linear region with 10% strain

**Table 2** Parameters of the DPD simulations for PLA/PEG blends

System	Chain length ( $N_{DPD}$ )		Composition (wt% PLA)	$\chi_{PLA-PEG}$	$a_{PLA-PEG}$
	PLA	PEG			
PLA/PEG 90:10	408	37	90	-0.59	23.09
PLA/PEG 80:20	408	37	80	-1.01	21.70
PLA/PEG 75:25	408	37	75	-0.59	23.07
PLA/PEG 70:30	408	37	70	-0.21	24.32
PLA/PEG 50:50	408	37	50	0.97	28.17
PLA/PEG 30:70	408	37	30	1.51	29.94
PLA/PEG 20:80	408	37	20	1.32	29.32
PLA/PEG 10:90	408	37	10	1.77	30.79

to determine the storage ( $G'$ ) and loss ( $G''$ ) moduli over a frequency range of 0.1–100 rad/s.

Dynamic viscoelastic properties of blend samples are carried out only at 180 °C since it was enough to cover the terminal region behavior.

## Results and discussion

### Flory-Huggins ( $\chi_{ij}$ ) parameters

A positive value of Flory-Huggins ( $\chi_{ij}$ ) parameters indicates immiscibility for blends of high molecular weight polymers. Generally, the critical value of  $\chi$  parameter ( $\chi_c$ ) was used to compare  $\chi_{ij}$  for predicting the miscibility of polymer blend.  $\chi_c$  of the polymer blend was calculated by:

$$\chi_c = \frac{1}{2} \left( \frac{1}{\sqrt{n_A}} - \frac{1}{\sqrt{n_B}} \right)^2 \tag{8}$$

where  $n_A$  and  $n_B$  represent the degree of polymerization of the pure polymers. If  $\chi_{ij}$  of the blend is smaller than  $\chi_c$ , the mixture is miscible. If  $\chi_{ij}$  is slightly larger than the  $\chi_c$ , the blend exhibits partial miscibility. For larger values of  $\chi_{ij}$ , the components are completely immiscible.

In this work, the degree of polymerization of PLA ( $n_{PLA}$ ) and PEG ( $n_{PEG}$ ) is 30 and 50, respectively. The obtained value of  $\chi_c$  is 0.053. The plot of  $\chi$  parameter of PLA/PEG blends versus weight fraction of PEG was displayed in Fig. 1. The calculated  $\chi$  parameter of polymer blends from MD simulation increases from -1.01 to 1.77 as a function of PEG content. The values of  $\chi_{PLA-PEG}$  parameter for PLA/PEG with PEG content of 10–30%wt are clearly below the  $\chi_c$  line, as shown in Fig. 1. This indicates that those PLA/PEG blends are completely miscible. On the other hand, for 50:50, 30:70,

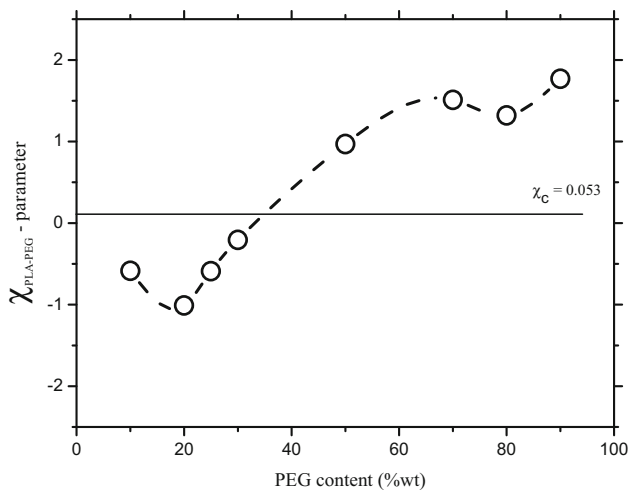


**Fig. 1** The plot of Flory-Huggins interaction parameter at different PEG contents

20:80, and 10/90 wt% PLA/PEG blends,  $\chi_{PLA-PEG}$  values are all above the  $\chi_c$  line, indicating immiscibility of PLA and PEG blends.

### Radial distribution functions

Radial distribution function,  $g(r)$ , is commonly used to characterize the molecular structure which gives the probability of finding a particle in the distance  $r$  from another particle. It is defined as:

$$g_{AB}(r) = \frac{1}{\rho_{AB} 4\pi r^2 \delta r} \frac{\sum_{t=1}^k \sum_{j=1}^{N_{AB}} \Delta N_{AB}(r \rightarrow r + \delta r)}{N_{AB} k} \tag{9}$$

where  $N_{AB}$  is the total number of atoms of A and B in the system,  $k$  is the number of time steps,  $\delta r$  is the distance interval,  $\Delta N_{AB}$  is the number of B (or A) atoms between  $r$  to  $r + \delta r$  around an A (or B) atom, and  $\rho_{AB}$  is the bulk density.

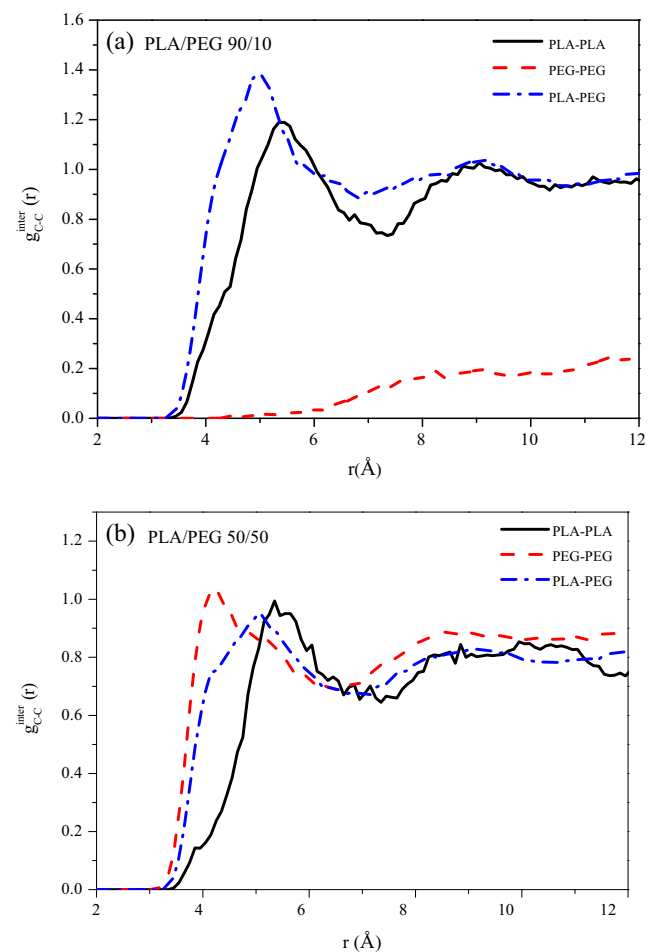


**Fig. 2** Radial distribution functions of the inter-molecular carbon-carbon pairs of PLA/PEG blends at different compositions of **a** 90:10 and **b** 50:50 wt%



**Fig. 3** Density profiles of the PLA/PEG blend for: **a** 90:10, **b** 80:20, **c** 70:30, **d** 50:50, **e** 30:70, and **f** 20:80 wt%

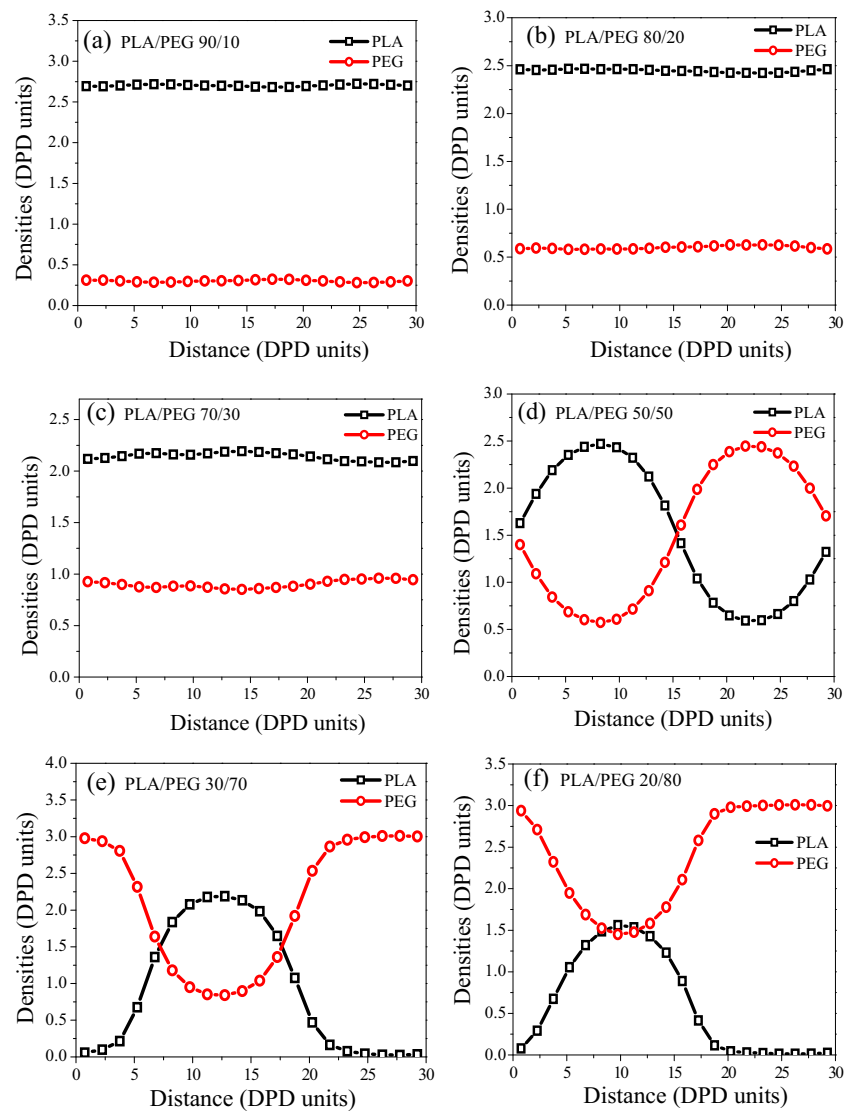


Figure 2 presents  $g(r)$  curves of inter-molecular carbon atomic pairs for PLA–PLA, PEG–PEG, and PEG–PLA chains for (a) 90:10 and (b) 50:50 wt% PLA/PEG blends. The inter-molecular distribution functions have been used to ascertain the degree of miscibility of polymer blends. When heterocontacts between the two components in the blends reach higher  $g(r)$  values than the contacts between the same components, miscibility occurs, whereas when this is not the case the system phase separates. For 90:10 wt% PLA/PEG blend,  $g(r)$  values of PLA–PLA and PEG–PEG are clearly lower than the  $g(r)$  value of PLA–PEG, indicating the PLA/PEG blend at this composition is miscible. This result was also observed for 80:20 and 70:30 wt% PLA/PEG blends (not shown here). In contrast, for other compositions (50:50, 30:70, 20:80, and 10:90 PLA/PEG blends), it is evident that  $g(r)$  values of PLA–PLA or PEG–PEG were higher than that PLA–PEG, implying that these polymer blends are immiscible.

### Density profiles

Figure 3 presents the density profiles distribution of PLA and PEG beads in the blends to study the composition dependence on the phase transition by DPD simulation. It is evident that the density distribution of PLA and PEG beads for 70:30 blends is still relatively constant. This result indicates that PLA and PEG up to this composition are well miscible. In contrast, the density values for the blends with PEG more than 30 wt% become highly fluctuated, indicating the tendency of phase separation. This observation implies that the 70:30 (wt/wt) composition is near the boundary of miscible and immiscible states of PLA/PEG blends.

### Polymer size

The root mean square (RMS) end-to-end distance of the polymer chains is an important structural property which is

generally used to describe the size or feature of the polymer chains in materials. Figure 4 shows the RMS end-to-end distance of PLA molecules in PLA/PEG blends with different PEG contents. It is evident that the RMS end-to-end distances of PLA molecules in the PLA/PEG blends decrease sharply in the range of 30–50 wt% of PEG concentration. The sketch represents the structural change of polymer chains in the blends. Mesoscopic morphology transits from homogeneous phase to phase separated morphologies at the composition about 70:30 (wt/wt) PLA/PEG blends. The size of PLA chains is decreased due to more confined boundary caused by phase separation in good accord with the observation of bead density change as described in “Density profiles.”

### Thermal behavior

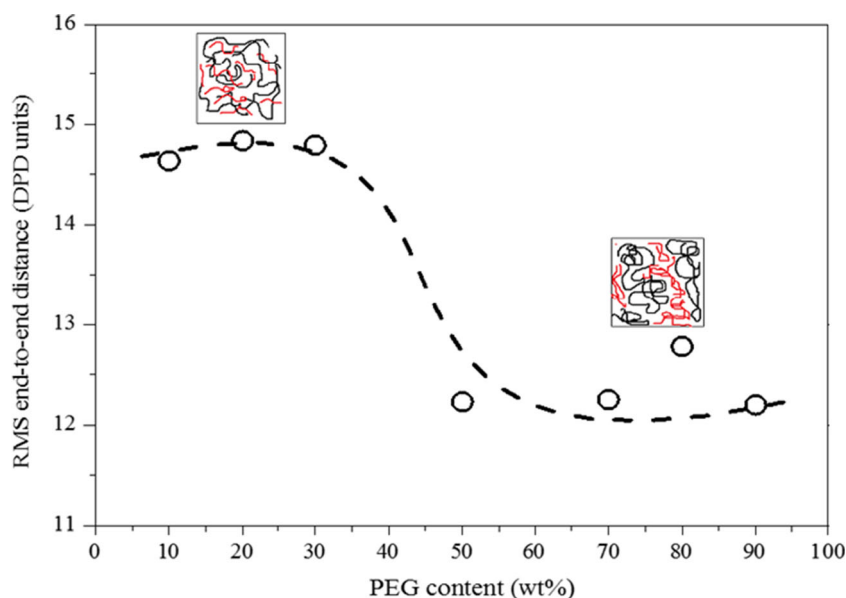
Thermal properties including the glass transition temperature ( $T_g$ ), crystallization temperature ( $T_c$ ), melting temperature ( $T_m$ ), degree of crystallinity ( $X_c$ ) of PLA, and PEG and their blends were investigated by DSC technique. These parameters were used to examine the miscibility of the blends. Thermograms of quenched PLA, PEG, and PLA/PEG blends are shown in Fig. 5. The quenched PLA was almost amorphous so that  $T_g$  at 51.8 °C can be clearly observed, followed by a small peak for enthalpy relaxation. The cold crystallization did not occur upon heating at 10 °C min<sup>-1</sup>, and consequently, very small and rather broad  $T_m$  peak exists at around 145 °C. The thermogram for PEG only shows  $T_m$  at 75 °C since  $T_g$  of PEG (ca. -60 °C) is below our experimental temperature. The  $T_g$  of PLA/PEG blends shifted to lower temperature with increase of PEG concentration and became not clear. However, with the existence of enthalpy relaxation, we can specify  $T_g$  only for PLA/PEG 90:10 and 80:20. For PLA/PEG (70:30) blend, it is very difficult to specify  $T_g$ . In

addition, another small peak exists beside the enthalpy relaxation peak close to  $T_m$  for PEG. This result may imply that this blend is phase separated (but it may not be concluded by this result alone). PLA/PEG with 10–30 wt% PEG displays a single  $T_g$  between those two pure components, reflecting that these samples are likely miscible. For PLA/PEG 50:50 sample,  $T_g$  is not observed but there are two endothermic peaks at 57.0 °C and at 149.2 °C corresponding to melting points of PEG and PLA, respectively. This observation implies that this blend is phase separated. The decreasing  $T_g$  and phase separation of PLA/PEG blends are consistent with previous studies [7, 8].

When these blends were heated at 10 °C/min, cold crystallization of PLA in the temperature range of 112–176 °C was observed. The cold crystallization temperature ( $T_c$ ) of PLA decreased slightly as PEG content increased in parallel with the shift in  $T_g$ . Subsequent melting temperature ( $T_m$ ) and crystallinity ( $X_c$ ) relative to PLA in the blend were slightly decreased for 10–30 wt% PEG content, but there is a large change in the PLA/PEG 50:50 system. Thermogram of PLA exhibits a single melting peak centered about 150 °C, whereas that of PLA/PEG with 10 and 20 wt% PEG was featured by a melting endotherm at 142–145 and ~150–151 °C. Thermal properties of all samples are shown in Table 3.

From DSC thermograms in Fig. 5, PLA/PEG blends are miscible in the melt for PEG content up to around 30 wt%. However, there were some reports that there is phase separation of PLA/PEG blends at room temperature due to slow PEG crystallization [7, 13]. Therefore, the slow cooling rate from the melt was performed to investigate the crystallization behavior of PEG component in the blends. Subsequent heating thermograms of PLA/PEG samples obtained from the cooling rate at 10 °C min<sup>-1</sup> from the melt are shown in Fig. 6. At this condition, the main characteristics of PLA/PEG

**Fig. 4** Simulated RMS end-to-end distance of PLA with different concentrations of PEG. The black color represents PLA chains, and red color represents PEG chains in the sketch



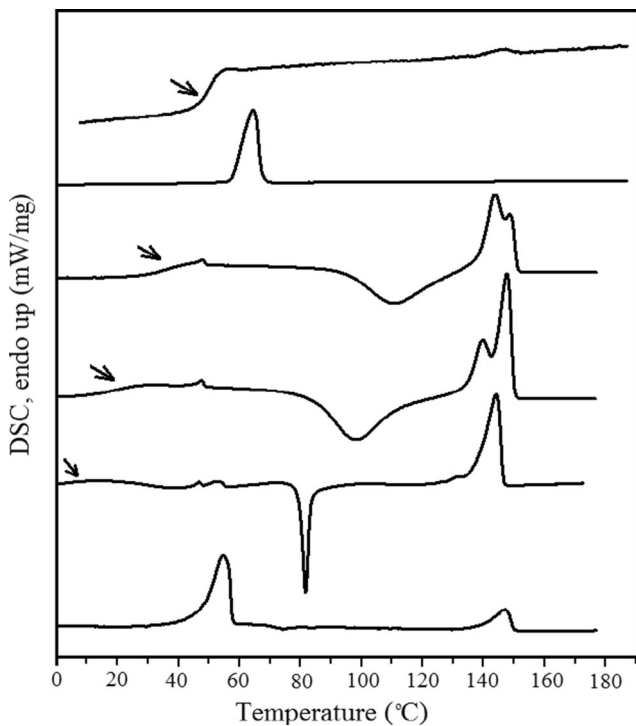


**Fig. 5** DSC thermograms of quenched samples of PLA, PEG, PLA/PEG 90:10, PLA/PEG 80:20, PLA/PEG 70:30, and PLA/PEG 50:50 blends from top to bottom, respectively, obtained with a heating rate of  $10\text{ }^{\circ}\text{C min}^{-1}$  (arrows denote the position of  $T_g$  and the small peak near  $T_g$ , around  $50^{\circ}$ , is the enthalpy relaxation)

blends with 10–20 wt% of PEG are quite similar to those in quench samples. The cooling rate from the melt does not have any effect on PEG crystallization in the mixture. As PEG is well dispersed in the amorphous region of PLA, PEG is difficult to crystallize. In contrast, PLA/PEG 70:30 sample showed two endothermic peaks at 57.9 and at  $150.1\text{ }^{\circ}\text{C}$  corresponding to the melting of PEG and PLA, respectively. This observation reflects that PEG can crystallize from the melt if

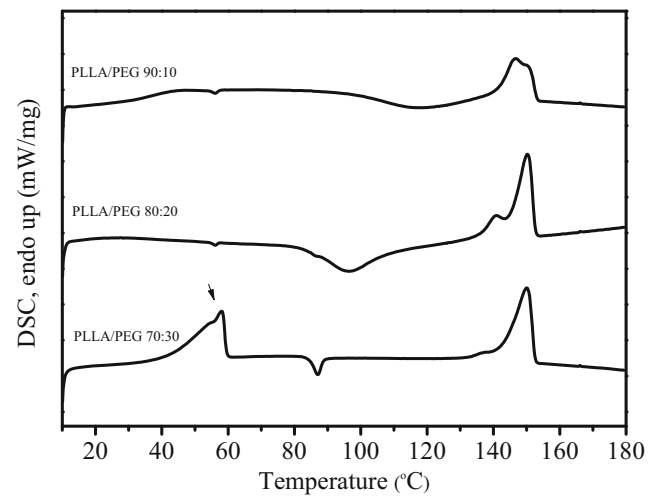


**Fig. 6** DSC thermograms for slowly cooled samples of PLA/PEG 90:10, PLA/PEG 80:20, and PLA/PEG 70:30 from top to bottom, respectively, obtained with a heating rate of  $10\text{ }^{\circ}\text{C min}^{-1}$

the cooling rate is slow enough and this leads to the phase separation. The ambiguity of data for quenched PLA/PEG 70:30 may be due to this effect.

### Rheological characterization

Double logarithmic plots of  $G'$  and  $G''$  vs  $\omega a_T$  for PLA/PEG blends at  $180\text{ }^{\circ}\text{C}$  are shown in Fig. 7. All polymer samples exhibit the rheological behavior of a typical polymer melt as characterized by smaller  $G'$  than the  $G''$ . As expected, the moduli of blend samples decreased with increasing PEG content. Frequency dependencies of  $G'$  and  $G''$  are close to  $\omega^2$  and  $\omega$ , respectively, denoting terminal region behavior. However, at low frequency ( $\omega < 5$ ) for PEG 25 and 30% samples, the  $G'$  data deviates from the characteristic slope of 2 in the terminal

**Table 3** Thermal properties of the PLA/PEG blends at a heating rate of  $10\text{ }^{\circ}\text{C min}^{-1}$

Sample	$T_g$ ( $^{\circ}\text{C}$ )	Cold crystallization		Melting		$X_c$ (%)
		$T_c$ ( $^{\circ}\text{C}$ )	$X_{cc}$ (%)	$T_m$ ( $^{\circ}\text{C}$ )		
				PEG	PLA	
PLA	51.8	–	–	–	149.8	0.50
PEG8k	–	–	–	66.7	–	–
PLA/PEG 90:10	37.4	112.5	39.1	–	145.9(151.2)	40.9
PLA/PEG 80:20	20.5	100.9	42.0	–	142.2(150.4)	43.7
PLA/PEG 70:30	9.3	85.9	18.6	–	150.0	39.7
PLA/PEG 50:50	–	76.4	4.7	57.0	149.2	29.1
PLA/PEG 90:10*	38.2	116.3	19.0	–	146.7	28.0
PLA/PEG 80:20*	15.9	96.5	27.8	–	150.0	44.0
PLA/PEG 70:30*	–	87.1	3.7	58.0	150.0	42.3

PLA/PEG 90:10\* indicates this system obtained from slow cool down from the melt  
138.4(149.7) refers to the first and second  $T_m$  peaks of PLA



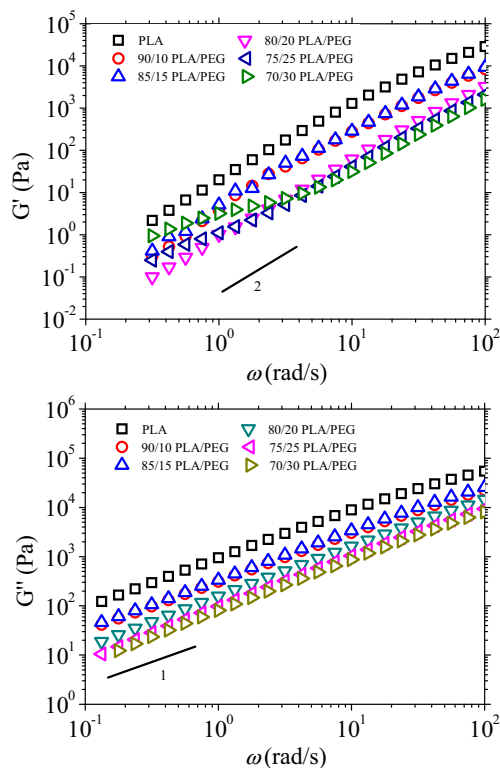


**Fig. 7** Log  $G'$  and log  $G''$  vs log  $\omega$  for PLA and PLA/PEG blends at 180 °C

region. There are two possibilities for the enhancement of moduli in the terminal region as described below.

In immiscible binary polymer blends, interface between two phases will be deformed and relaxed during the rheological measurements. The interfacial tension acts as excess stress reflecting the deformation and relaxation of interface, depending on many parameters [34]. Another possibility is concentration fluctuation in the miscible blends [35]. The fluctuation generally becomes larger and its lifetime becomes longer near the phase separation point. When two components have big difference in their viscoelastic properties, concentration fluctuation causes large dynamic heterogeneity of the system. If the applied flow cannot dissipate the fluctuation, the resulting rheological data become similar to that of heterogeneous system even there is no interface.

It should be remarked that one cannot specify whether the lower frequency dependence of  $G'$  is due to concentration fluctuation or phase separation by considering only the result shown in Fig. 7. Nevertheless, the data strongly suggest that PEG 25 and 30% at 180 °C is close to the phase separation point, consistent with the DSC results.

## Conclusion

MD and DPD simulations were employed to predict the miscibility of PLA/PEG systems. The  $\chi_{ij}$  parameter for PLA/PEG

blends with different PEG contents were calculated by MD simulation. The PEG concentrations of 10 to 90 wt% were varied to blend with PLA. The  $\chi_{ij}$  parameter of polymer mixtures was analyzed to determine the miscibility of PLA/PEG blends. The results show that PLA and PEG are miscible at low PEG concentrations (10–30 wt%), while at high PEG concentration (>50 wt%) the immiscibility was observed.

Bead density distribution of PLA and PEG in the blends was also calculated by DPD simulation to determine the miscibility of PLA/PEG blends. The density profiles of the blends exhibit homogeneous phase at the PEG content of 10–30 wt% and exhibit phase separation at higher PEG contents. The finding results agree well with the results from MD simulations. In addition, the density fluctuation of PLA and PEG beads was clearly detected at the 70:30 PLA/PEG. The chain dimensions of PLA were investigated by determining the end-to-end distance with different PEG contents. The result shows that the chain dimensions of PLA decrease when the PEG content increase which leads to the phase separation of PLA and PEG.

The miscibility of PLA/PEG blends was also investigated by a combination of DSC and rheological techniques. DSC thermograms of 90:10, 80:20, and 70:30 PLA/PEG show single  $T_g$  and PLA melting peak, indicating PLA/PEG is miscible over this composition, while phase separation was seen in PLA/PEG 50:50 (wt/wt) blends. This finding result is consistent to the miscibility prediction from computer simulation. Rheological measurement of PLA/PEG, performed at the melt state, showed deviation of slope of  $G'$  curve at low frequency region from 2 for PLA/PEG at 75:25 and 70:30 (wt/wt), indicating that these mixture are near the phase separation points at 180 °C.

**Acknowledgments** The financial support for this work by the Commission on Higher Education, Ministry of Education (Thailand) for supporting the grant fund under the program Strategic Scholarships for Frontier Research Network for the Ph.D. Program is gratefully acknowledged. All molecular simulation works were done at Suranaree University of Technology (SUT), Thailand, and most of the experimental part was performed at Kyushu University, Japan. A.T. and V.V. would like to thank National Nanotechnology Center, Thailand, for their permission to use Material Studio software. V.V. thanks the support of the Advanced Organic Materials Research Group, SUT.

## References

1. Auras R, Lim LT, Selke SEM, Tsuji H (2010) Poly(lactic acid): synthesis, structures, properties, processing and applications. Wiley, Canada
2. Garlotta D (2001) A literature review of poly(lactic acid). J Polym Environ 2(9):63–84
3. Eguiburu JL, Iruin JJ, Fernandez-Berridi MJ, Roman JS (1998) Blends of amorphous and crystalline poly(lactides) with poly(methyl methacrylate) and poly(methyl acrylate): a miscibility study. Polymer 39:6891

4. Kulinsky Z, Piorkowska E (2005) Crystallization, structure and properties of plasticized poly(L-lactide). *Polymer* 46:10290–10300
5. Ljungberg N, Wesslen B (2002) Tributyl oligomers as plasticizers for poly (lactic acid): thermo-mechanical film properties and aging. *Polymer* 44:7679–7688
6. Venkatraman SS, Jie P, Min F, Freddy BYC, Leong-Huat G (2005) Micelle-like nanoparticle of PLA-PEG-PLA triblock copolymer as chemotherapeutic carrier. *Int J Pharm* 298:219–232
7. Hu Y, Hu YS, Topolkaev V, Hiltner A, Baer E (2003) Crystallization and phase separation in blends of high stereoregular poly(lactide) with poly(ethylene glycol). *Polymer* 44:5681–5689
8. Lai WC, Liao WB, Lin TT (2004) The effect of end groups of PEG on the crystallization behaviors of binary crystalline polymer blends PEG/PLLA. *Polymer* 45:3037–3080
9. Kulinski Z, Piorkowska E, Gadzinowska K, Stasiak M (2006) Plasticization of poly(L-lactide) with poly(propylene glycol). *Biomacromolecules* 7:2128–2135
10. Jacobsen S, Fritz HG (1999) Plasticizing polylactide the effect of different plasticizers on the mechanical properties. *Polym Eng Sci* 39:1303–1310
11. Pillin I, Montrelay N, Grohen Y (2006) Thermo-mechanical characterization of plasticized PLA: is the miscibility the only significant factor? *Polymer* 47:4676–4682
12. Hu Y, Rogunova M, Topolkaev V, Hiltner A, Baer E (2003) Aging of poly(lactide)/poly(ethylene glycol) blends: part 1. Poly(lactide) with low stereo-regularity. *Polymer* 44:5701–5710
13. Kulinski Z, Piorkowska E (2005) Crystallization, structure and properties of plasticized poly(L-lactide). *Polymer* 46:10290–10300
14. Sheth M, Kumar RA, Dave E, Gross RA, McCarthy SP (1997) Biodegradable polymer blends of poly (lactic acid) and poly(ethylene glycol). *J Appl Polym Sci* 66:1495–1505
15. Younes H, Cohn C (1988) Phase separation in poly(ethylene glycol)/poly(lactic acid) blends. *Eur Polym J* 8:765–773
16. Glotzer SC, Paul W (2002) Molecular and mesoscale simulation methods for polymer materials. *Annu Rev Mater Res* 32:401–436
17. Jawalkar SS, Adoor SG, Sairam M, Nadagouda MN, Aminabhavi TM (2005) Molecular modeling on the binary blend compatibility of poly(vinyl alcohol) and poly(methyl methacrylate): an atomistic simulation and thermodynamic approach. *J Phys Chem B* 109:15611–15620
18. Jawalkar SS, Aminabhavi TM (2006) Molecular modeling simulations and thermodynamic approaches to investigate compatibility/incompatibility of poly(l-lactide) and poly(vinyl alcohol) blends. *Polymer* 47:8061–8071
19. Jawalkar SS, Kothapalli VSN, Halligudi SB, Malladi S, Aminabhavi TM (2007) Molecular modeling simulations to predict compatibility of poly(vinyl alcohol) and chitosan blends: a comparison with experiments. *J Phys Chem B* 111:2431–2439
20. Mu D, Huang XR, Lu ZY, Sun CC (2008) Computer simulation study on the compatibility of poly(ethylene oxide)/poly(methyl methacrylate) blends. *Chem Phys* 348:122–129
21. Gai JG, Li HL, Schrauwen C, Hu GH (2009) Dissipative particle dynamics study on the phase morphologies of the ultrahigh molecular weight polyethylene/polypropylene/poly(ethylene glycol) blends. *Polymer* 50:336–346
22. Luo ZL, Jiang JW (2010) Molecular dynamics and dissipative particle dynamics simulations for the miscibility of poly(ethylene oxide)/poly(vinyl chloride) blends. *Polymer* 51:291–299
23. Yin Q, Luo JH, Zhou G, Yin QJ, Jiang B (2010) A molecular simulation of the compatibility of chitosan and poly(vinyl pyrrolidone). *Mol Simul* 36:186–191
24. de Arenaza IM, Meaurio E, Coto B, Jose-Ramon Sarasua JR (2010) Molecular dynamics modelling for the analysis and prediction of miscibility in polylactide/polyvinilphenol blends. *Polymer* 51:4431–4438
25. Fu YZ, Liao LQ, Lan YH, Yang LX, Mei LY, Liu YQ, Hu SQ (2012) Molecular dynamics and mesoscopic dynamics simulations for prediction of miscibility in polypropylene/polyamide-11 blends. *J of Mol Structure* 1012:113–118
26. Gu GH, Gu HY, Lang MD (2013) Molecular simulation to predict miscibility and phase separation behavior of chitosan/poly( $\epsilon$ -caprolactone) binary blends: a comparison with experiments. *Macromol Theory Simul* 22:377–384
27. Fu YZ, Liao LQ, Yang LX, Lan YH, Mei LY, Liu YQ, Hu SQ (2013) Molecular dynamics and dissipative particle dynamics simulations for prediction of miscibility in polyethylene terephthalate/polylactide blends. *Mol Simul* 39:415–422
28. Rakkapao N, Visit Vao-soongnern V (2014) Molecular simulation and experimental studies of the miscibility of chitosan/poly(ethylene oxide) blends. *J Polym Res* 21:606–615
29. Flory PJ (1989) *Statistical mechanics of chain molecules*. Hanser, Germany
30. Theodorou DN, Suter UW (1986) Atomistic modeling of mechanical properties of polymeric glasses. *Macromolecules* 19:139–154
31. Meirovitch H (1983) Computer simulation of self-avoiding walks: testing the scanning method. *J Chem Phys* 79:502
32. Hoogerbrugge PJ, Koelman JMVA (1992) Simulating microscopic hydrodynamic phenomena with dissipative particle dynamics. *Europhys Lett* 19:155–160
33. Groot RD, Warren PB (1997) Dissipative particle dynamics: bridging the gap between atomistic and mesoscopic simulation. *The Journal of Chemical Physical* 107:4423–4435
34. Kitade S, Ichikawa A, Imura N, Takahashi Y, Noda I (1997) Rheological properties and domain structures of immiscible polymer blends under steady and oscillatory shear flows. *J Rheol* 41:1039–1060
35. Takahashi Y, Ojika Y, Akazawa Y, Takano A, Matsushita Y (2007) Fluctuation effects on viscoelastic properties of Diblock copolymer solutions in disordered state. *Polym J* 39:509–513